Applied Catalysis A, General 698 (2025) 120238

Contents lists available at ScienceDirect

Applied Catalysis A, General

journal homepage: www.elsevier.com/locate/apcata

Selective production of levulinic acid from furfuryl alcohol over acid-modified zeolite catalysts

Laura Fuentes-Rodríguez, Adrien Le Corre, Yolanda Cesteros *

Universitat Rovira i Vigili, Departament de Química Física i Inorgànica, C/ Marcel·lí Domingo, 1, Tarragona 43007, Spain

ARTICLE INFO

Keywords:
Acid-modified zeolites
BrØnsted acidity
Catalysis
Furfuryl alcohol
Levulinic acid

ABSTRACT

Commercial zeolites (Na-ZSM-5, NH_4-βeta, and Na-mordenite) were protonated, and sulfonic-acid functionalized through microwave-assisted methods to be applied as acid catalysts for the selective production of levulinic acid from furfuryl alcohol using acetone-water mixture as greener solvent. Sulfonated zeolites enhanced levulinic acid formation due to their higher amount of more accessible BrØnsted acid sites. The different zeolite structure of the catalysts clearly affected the accessibility of the reagents to the acid sites, especially for the one-dimensional H-mordenite catalyst, which showed null selectivity to levulinic acid. Interestingly, this effect was in part overcome by the sulfonic-acid functionalization of mordenite increasing considerably its selectivity to levulinic acid up to 40 %. This means that sulfonation mainly occurred on the external zeolite surface. Sulfonated βeta catalyst showed the highest selectivity to levulinic acid (76 %) for a complete conversion while H-βeta had higher reuse stability since deactivating products adsorbed during reaction can be eliminated by calcination.

1. Introduction

In recent years, there has been a growing interest in producing chemicals from residual biomass, as this carbon source does not compete with biomass intended for human consumption. This approach has a lower environmental impact, enabling the production of high-value-added chemicals and helping to reduce and mitigate the effects of fossil fuels [1–3].

Levulinic acid (LA) is considered one of the 12 most valuable platform chemicals derived from biomass [4], as it serves as a precursor to high-value-added products such as fuel additives (γ-valerolactone, levulinate esters, etc.) [5–10], fertilizers (5-aminolevulinic acid) [11,12], and resin precursors (diphenolic acid) [13]. LA can be obtained through acid catalysis from furfuryl alcohol (FOL), which is obtained from furfural derived from lignocellulosic materials [14,15]. The catalytic production of levulinic acid from furfuryl alcohol involves the hydration and ring-opening of furan. However, undesirable side reactions, such as the dehydration of the furan ring to form 4-hydroxy-2-cyclopentenone (2-HCP) or the formation of furan resins, also called humins, are usually additionally obtained due to the high reactivity of FOL (Scheme 1) [16–19].

Traditionally, homogeneous acid catalysts such as H_2SO_4, HCl, or HBr have been used to produce LA [17,19,20]. However, this method has several disadvantages, including toxicity, handling risks, and infrastructure requirements for proper use. Additionally, FOL easily polymerizes in acidic aqueous media, which decreases the reaction yield [21–25]. Some alternatives to prevent polymerization include reducing the concentration of FOL or using an organic solvent.

In recent years, heterogeneous acid catalysts have been explored as a more environmentally friendly alternative. LA yields of 60–70 % from FOL have been reported using different H-zeolites as catalysts at 120ºC. However, this involved the use of highly polluting solvents like tetrahydrofuran (THF), an organic solvent that does not promote polymerization when mixed with water [26].

More recently, environmentally benign solvent systems such as methyl ethyl ketone (MEK), acetone and cyclopentyl methyl ether (CPME) have been employed, primarily using H-ZSM-5 (Si/Al= 50) as a catalyst, achieving LA yields of 58 %, 32 % and 11 %, respectively [27]. Other zeolites like H-βeta or ultrastable zeolite in addition to other types of catalysts, such as ion-exchange resins (Amberlyst), heteropolyacid-type super acid, or sulfated zirconia superacid, were also used, all with poorer results [27]. Guzmán et al. concluded that the use of moderate H_2 pressures (10–15 bar) prevented polymerization reactions [27]. The introduction of mesopores and few Al sites in straight and sinusoidal channels of ZSM-5 by an alkaline treatment of the commercial zeolite followed by an acid treatment improved the LA yield to

* Correspondence to: Department Química Física i Inorgànica, Universitat Rovira i Virgili, C/Marcel·lí Domingo 1, Tarragona 43007, Spain.
E-mail address: yolanda.cesteros@urv.cat (Y. Cesteros).

https://doi.org/10.1016/j.apcata.2025.120238
Received 4 January 2025; Received in revised form 13 March 2025; Accepted 22 March 2025
Available online 24 March 2025

76 % at 120 ºC using an acetone/water solvent mixture [28]. Furthermore, other catalysts, such as SO_3H silica nanoflowers in γ-valerolactone (GVL) mixed with water were reported, achieving LA yield of 90 % at 120 ºC for 2.5 h [29], indicating that sulfonated materials could be a promising alternative.

The aim of this work is to study the use of various acid-modified zeolite materials as catalysts for the conversion of furfuryl alcohol into levulinic acid using a greener solvent. Special attention will be paid to study the effect of the structure, surface and acid properties of the catalysts on the catalytic reaction.

2. Experimental section

2.1. Catalysts preparation

Microwave-assisted (Flexiwave, Milestone) sulfonic-acid functionalization of the zeolite NH_4-βeta (Si/Al=12.5) from Zeolyst international, Na-ZSM-5 (Si/Al= 20) from Akzo Nobel, and Na-Mordenite (Si/Al=6.5) from Zeolyst international were carried out using the appropriate amounts of 2-(4-chlorosulfonylphenyl) ethyltrimethoxysilane (CSPTMS) solution in methylene chloride (50 wt%, Gelest) in 2 M HCl solution by refluxing with microwaves at 40 ºC for 2 h. Samples were filtered, washed with deionised water and dried overnight (S-βeta, S-ZSM-5, S-Mordenite).

βeta, Mordenite and ZSM-5 zeolites were also protonated. For this purpose, ZSM-5 and Mordenite were treated with an aqueous solution of 1 M NH_4NO_3 (Sigma-Aldrich) at 100 ºC for 1 h and subsequently washed with distilled water. Afterwards, both zeolites together with NH_4-βeta were calcined at 540 ºC for 5 h to obtain H-βeta, H-Mordenite and H-ZSM-5 catalysts.

2.2. Characterization of catalysts

Catalysts were characterized by X-ray diffraction (XRD) patterns of the samples were obtained with a Siemens D5000 diffractometer using nickel-filtered Cu Kα radiation. Samples were dusted on double-sided sticky tape and mounted on glass microscope slides. The patterns were recorded over a range of 2θ angles from 5° to 40° and crystalline phases were identified using the Joint Committee on Powder Diffraction Standards (JCPDS) files (48–0074 βeta, 37–359 ZSM-5 and 43–0171 Mordenite). Crystallinity of the acid-modified mordenites was determined by comparing the sum of the peak areas of (150), (202), (350) and (402) (22–32º 2θ) with respect to commercial Na-mordenite. Crystallinity of the acid-modified ZSM-5 samples was calculated using the (051) peak intensity compared with the commercial zeolite sample. The integrated intensity of the signal at $2\theta = 22.4^{\circ}$ was used to evaluate the crystallinity of beta samples.

N_2 physisorption adsorption–desorption characterization was performed using a 3FLEX Micromeritics equipment at −196 ºC. Before measurements all samples were outgassed at 300 ºC for 6 h. The BET specific surface areas were calculated using adsorption data in the relative pressure range $0 < P/P_0 < 0.1$ ($\sigma N_2 = 0.162\ nm^2$). External surface areas were obtained by t-plot analysis of the adsorption data in the $3.5 \leq t \leq 5$ Å t range by adopting the de Boer reference isotherm equation.

SEM was used to observe the morphology and particle sizes of the samples. Experiments were performed on a scanning electron microscope, JEOL JSM6400, operating at accelerating voltage of 25 kV and work distances of 10 mm, and magnifications of 10.000X. This equipment also has an Energy Dispersive X-ray Spectroscopy detector (EDX), which was used for mapping the sulfur present in the spent and fresh S-βeta catalyst.

Elemental ratio of Si/Al analyses of the samples were obtained by X-ray fluorescence (XRF) with a Philips PW-2400 sequential analyzer with Philips Super Q software. All measurements were performed by triplicate.

Thermogravimetric analyses (TGA) were performed with a Mettler Toledo TGA 2 equipment from 50 ºC to 800 ºC at 10 °C/min under airflow to calculate the sulfur content of the sulfonic acid-functionalized zeolites, and to characterize some spent catalysts with respect to the fresh ones.

Acid capacity of sulfonated zeolites was measured by the determination of cation exchange capacity using 2 M aqueous sodium chloride solution as cationic-exchange agent. The released protons were then potentiometrically titrated using NaOH (0.01 M) and phenolphthalein as a indicator. In the case of H-zeolites, the acidity was measured using standard methods based on cyclohexylamine desorption [30–32]. Samples were exposed to liquid cyclohexylamine at room temperature, rested overnight, and heated in an oven at 80 ºC for 2 h to allow base permeation [30–32]. The temperature was then raised to 250 ºC for 2 h to remove the physisorbed cyclohexylamine. TGA desorption curves were recorded using a Mettler Toledo TGA 2 equipment. Samples were heated from 50 to 700 ºC at 10 ºC/min under nitrogen flow (25 mL/min). Weight loss from base desorption was used to calculate acid content in mmol of cyclohexylamine per gram, assuming one mole of cyclohexylamine equals one mole of protons [30–32].

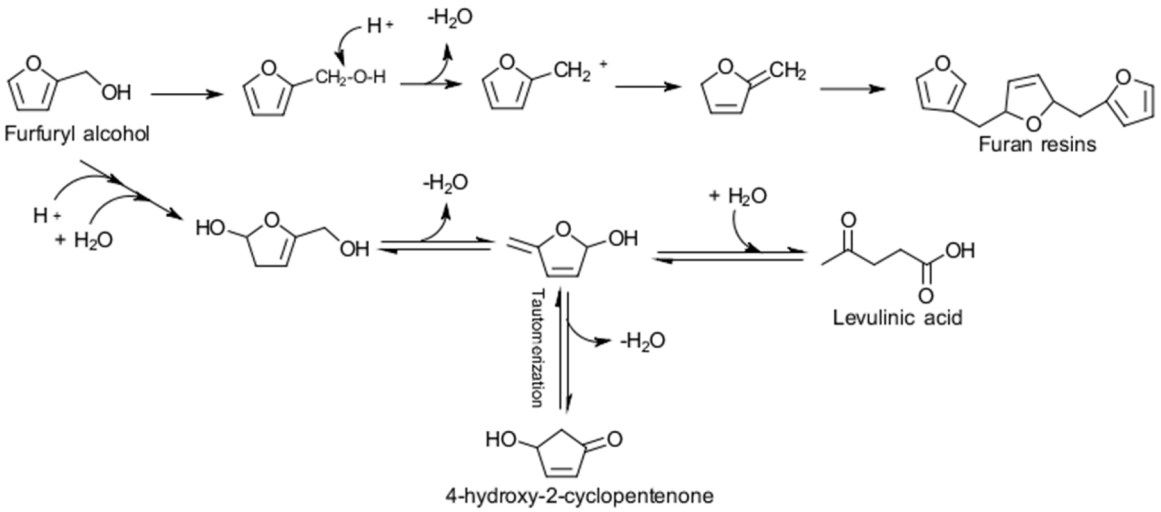

Scheme 1. Main reactions of furfuryl alcohol catalyzed by BrØnsted acid sites.

2.3. Catalytic activity

The catalytic activity was evaluated in a batch reactor using 0.14 g of furfuryl alcohol (98 %, Sigma-Aldrich), 20 mL of water/acetone solvent with a ratio of 1:9, 700 rpm, 0.2 g of catalyst at 120 ºC for 1 h. After purging with N_2, 15 bars of H_2 were added. The reaction products were analysed by gas chromatography (GC) using a chromatograh model Shimadzu GC-2010 equipped with a SupraWax-280 column and a FID detector. Furfuryl alcohol conversion and selectivity to levulinic acid (Sigma-Aldrich) were determined from calibration lines obtained from commercial products, 1-butanol (Sigma-Aldrich) was used as internal standard. 4-hydroxy-2-cyclopentanone was identified using the commercial product (98 %, Cymit). The FOL conversion and the selectivity towards levulinic acid were calculated using the following equations:

$$\%\ \text{Conversion} = \frac{\text{number of moles of converted furfuryl alcohol}}{\text{number of moles of initial furfuryl alcohol}} \times 100$$

$$\%\ \text{Selectivity to LA} = \frac{\text{number of moles of FOL converted to levulinic acid}}{\text{number of moles of converted furfuryl alcohol}} \times 100$$

3. Results and discussion

3.1. Characterization of catalysts

Acid-modified zeolites maintained the structure of their corresponding parent zeolite although some decrease of crystallinity was observed by XRD (Table 1), especially for the sulfonated samples, since a decrease in the intensity and some broadening of the XRD peaks was observed (Fig. 1). The harshest treatment of the acid-sulfonic functionalization justifies the slight lower crystallinity observed for these samples.

N_2 adsorption-desorption isotherms of commercial and acid-modified zeolites were of type I (Fig. 2), which correspond to microporous materials, according to the Brunauer, Deming, Deming and Teller classification [33]. ZSM-5 samples showed a relatively steep

of nitrogen adsorption at partial pressures up to $P/P_0 = 0.2$, which has been related to phase

transition of N_2 between different pore sizes [34], although a close packing of the nitrogen molecules at the intersections of the channels has also been suggested [35]. The nitrogen isotherms of beta samples showed a minor contribution of the type IV isotherm with a hysteresis loop between 0.8 and 0.9 P/P_0 indicating the presence of small fraction of mesopororesres. This could be related to the presence of stacking faults in the structure of this zeolite [36].

All protonated samples showed slightly higher BET area and external surface area values than those of the corresponding commercial zeolites (Table 1). This can be related to the slight dealumination suffered by these protonated samples, as observed by XRF (Table 1), due to the temperature used during calcination, as reported by other authors [37].

Regarding microwave-assisted sulfonic-acid functionalized samples, S-βeta showed higher dealumination than S-mordenite, and S-Mordenite higher than S-ZSM-5, as deduced from XRF results (Table 1). The more flexible the zeolitic structure is, the easier it can be dealuminated [38]. βeta, which is formed by a three-dimensional 12-ring pore system with straight channels of diameter 6.6 × 6.7 Å and sinusoidal channels of diameter 5.6 × 5.6 Å, has a more flexible zeolitic structure than mordenite, which has a one-dimensional pore system with 12-ring channels of diameter 6.7 × 7.0 Å and compressed 8-ring channels of diameter 2.6 × 5.7 Å, while ZSM-5 has a three-dimensional 10-ring pore system with channels of diameter 5.1 × 5.5 Å. Additionally, zeolite βeta has many structure stacking faults [36], as commented above, while mordenite, although less frequently, may also have. The presence of these structural defects can favor dealumination [38]. Thus, ZSM-5 has the most stable structure, explaining its lower dealumination (Table 1).

S-βeta and S-ZSM-5 exhibited significant lower BET and lower external surface areas than those of commercial βeta and ZSM-5, respectively (Table 1, Fig. 2). In contrast, S-Mordenite had higher BET and external surface areas than commercial mordenite (Table 1, Fig. 2). Several factors can contribute to explain these variations: the loss of the zeolite crystallinity, observed by XRD (Fig. 1), the partial dealumination of the sulfonated zeolites (Table 1), which depend on the zeolite structure and is a consequence of the acidic medium used during sulfonation, and the fact that pores can be partially blocked by the incorporated sulfonic groups. Thus, the increase of surface area observed after sulfonation of mordenite can be mainly attributed to the higher mesoporosity generated because of the partial dealumination of this zeolite, as reported before [38,39], while the decrease of surface area observed for sulfonated βeta and ZSM-5 samples should be related to the loss of crystallinity together with the incorporation of the sulfonic acid groups in the zeolite framework.

Interestingly, the loss of aluminum during the sulfonation treatment

Table 1
Characterization of the acid-modified microporous catalysts.

Catalyst	Crystallinity (%)[a]	Si/Al (XRF)	BET Surface area (m^2/g)	t-plot External surface area (m^2/g)	Sulfur content[b]	Acid capacity (mmol H^+/g)
NH_4-βeta	100	12.5	630	190	–	–
Na-ZSM−5	100	20.0	505	26	–	–
Na-Mordenite	100	6.5	303	31	–	–
H-βeta	89	13.7	636	214	–	0.60[c]
H-ZSM−5	100	20.2	510	93	–	0.37[c]
H-Mordenite	93	6.9	312	38	–	0.18[c]
S-βeta	45	71.3	333	183	0.71	0.74[d]
S-ZSM−5	54	28.6	263	79	0.68	0.52[d]
S-Mordenite	31	26.4	433	58	0.63	0.80[d]

[a] Calculated from XRD;
[b] (mmol organic sulfonic acid group/g sample) calculated by TGA.
[c] Obtained by TGA of adsorbed cyclohexylamine.
[d] Determined by potentiometric titration.

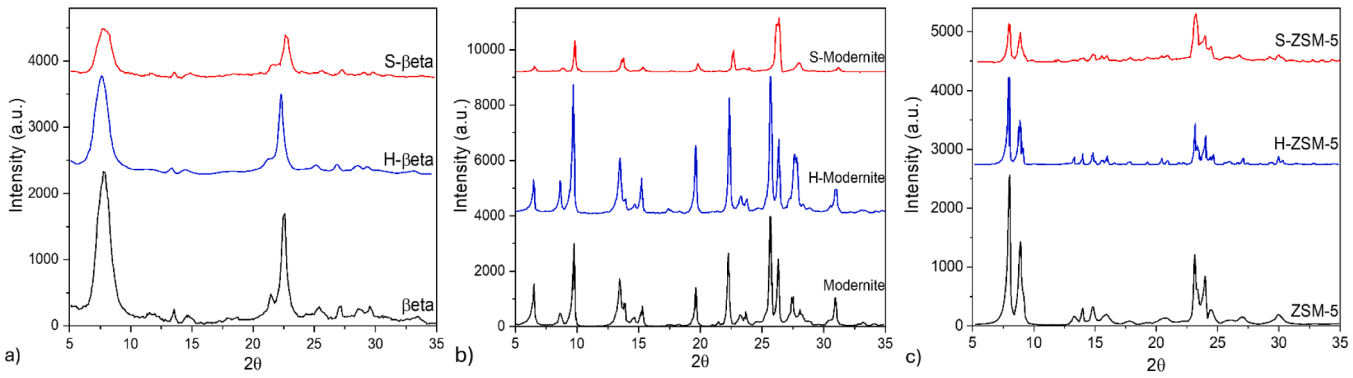

Fig. 1. XRD patters of a) βeta, H-βeta and S-βeta b) ZSM-5, H-ZSM-5 and S-ZSM-5, c) Mordenite, H-Mordenite and S-Mordenite.

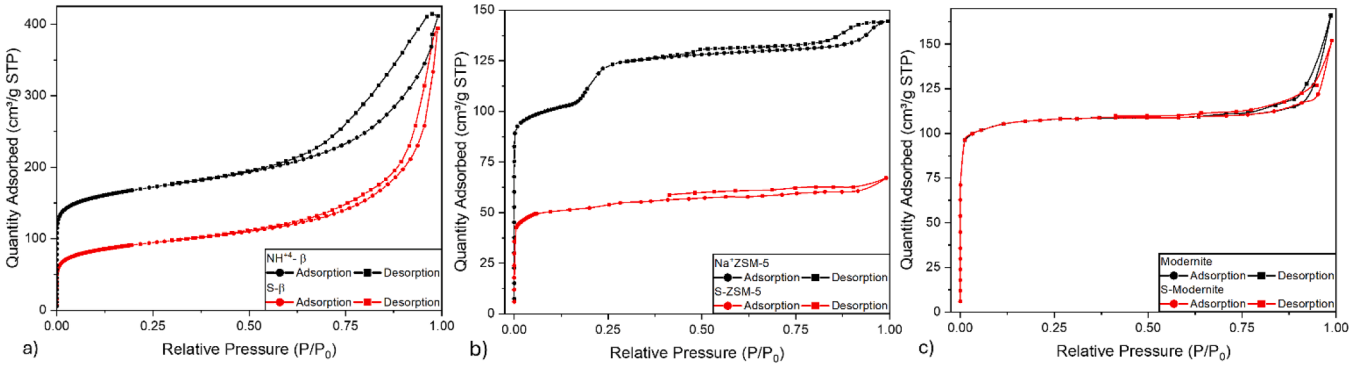

Fig. 2. N_2 adsorption-desorption isotherms a) βeta and S-βeta b) ZSM-5 and S-ZSM-5 c) Mordenite and S-Mordenite.

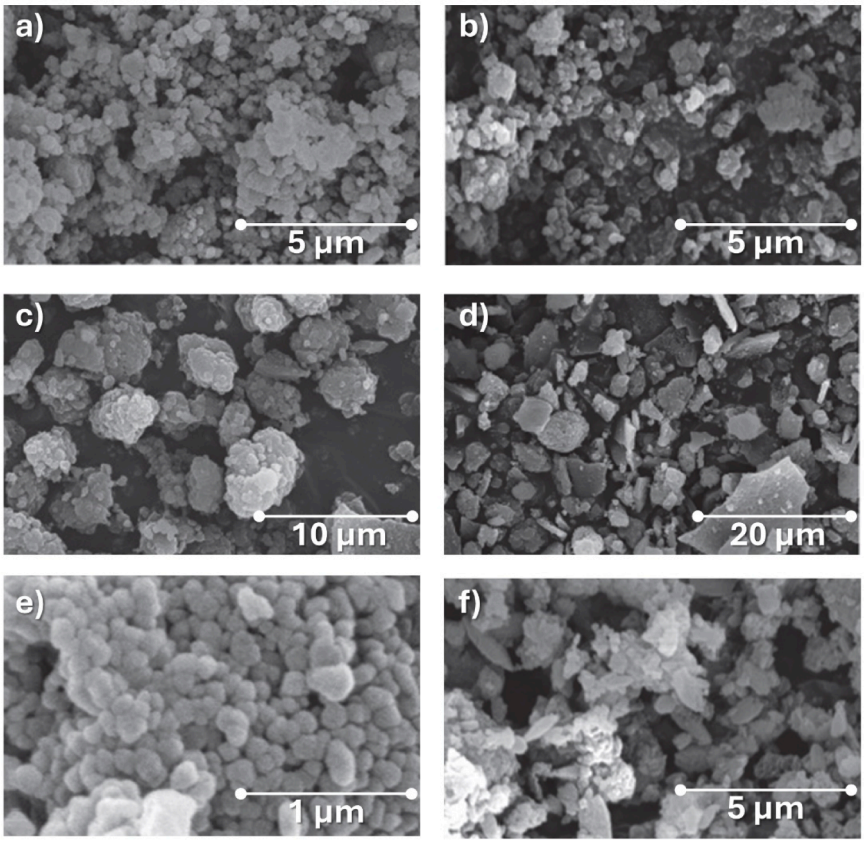

Fig. 3. SEM of catalysts a) βeta, b) S-βeta, c) ZSM-5, d) S-ZSM-5, e) Mordenite and f) S-Mordenite.

led to the formation of additional silanols that can react with the sulfonating agent, increasing the amount of H^+ in S-zeolites with respect to the H-zeolites. This explains the higher acidity of the sulfonated catalysts, in agreement with the sulfur content calculated by TGA (Table 1).

Scanning electron microscopy was used to monitor the morphologies and sizes of the particles of the sulfonic acid-functionalized S-βeta, S-ZSM-5 and S-Mordenite with respect to their corresponding commercial zeolites (Fig. 3). S-βeta and S-Mordenite samples appeared less agglomerated, with less densely packed crystallites, than their corresponding commercial ones. Besides, the micrographs of ZSM-5 samples were very similar.

3.2. Catalytic activity

Fig. 4 shows the catalytic activity results of the acid-modified zeolites for the conversion of furfuryl alcohol (FOL) at 120 °C, 15 bar of H_2 for 1 h using a water/acetone ratio of 1:9 as green solvent. Acetone was used due to the ability of ketone groups to inhibit humin formation [17,27,28], ensuring the catalytic surface remains accessible. Furthermore, its miscibility with water allows for the creation of a homogeneous reaction medium, enhancing interactions between the reactants and the catalyst. Small amounts of water are essential for controlling reaction kinetics and favor hydrolysis of FOL [17,27,28]. Wang et al. optimized the water/acetone ratio at 1:9 for this reaction [28].

Conversion was complete for all catalysts except for H-Mordenite (Fig. 4). These total conversion values agreed with previous results reported for this reaction because of the high reactivity of FOL [26–29]. The lower conversion of H-Mordenite may be explained by the lower accessibility of the reagents to the active sites in the one-dimensional pore structure of mordenite when compared with βeta and ZSM-5 samples, which have three-dimensional pore structure. Additionally, H-Mordenite had the lowest external surface area (Table 1).

Regarding selectivity values, H-βeta and H-ZSM-5 catalysts showed moderate selectivity to levulinic acid (52–58 %) (Fig. 4). This can be related to the amount of BrØnsted acid sites present in these catalysts (Table 1). It is interesting to remark that the selectivity to LA was slightly higher for H-ZSM-5 having less amount of BrØnsted acid centers and lower external surface area than H-βeta (Table 1). This confirms the effect of the structural characteristics of the catalyst, affecting accessibility, in addition to the acidity for this reaction, as proposed by other authors [28]. In contrast, for H-Mordenite, LA was not detected. This was the catalyst with the lowest amount of BrØnsted acid sites, lowest external surface area (Table 1) and with a less flexible and less accessible one-dimensional pore structure.

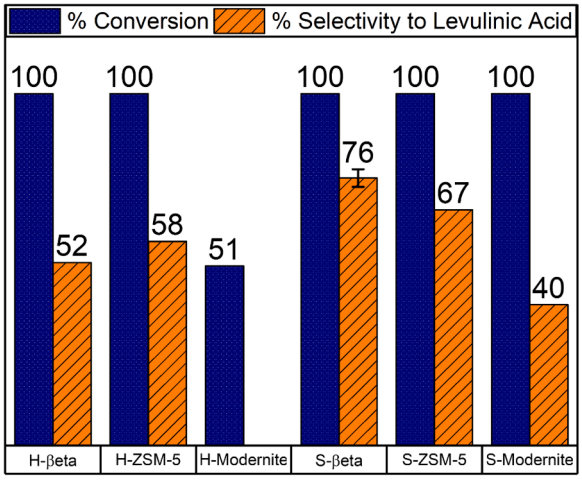

Fig. 4. Catalytic activity for the conversion of furfuryl alcohol to levulinic acid. Reaction conditions: solvent: water/acetone ratio of 1:9, 0.2 g of catalyst at 120 °C, 15 bar H_2 for 1 h. Error bar is indicated for the best catalyst.

A significant increase in LA formation for a total conversion was observed for all sulfonated zeolites when tested at the same reaction conditions than H-zeolites. This can be related to the higher amount of BrØnsted acid sites, due to the incorporation of the sulfonic groups (Table 1). Interestingly, the negative effect of the zeolite structure observed with H-Mordenite catalyst was in part overcome by the sulfonic-acid functionalization of mordenite since a considerable increase in the selectivity to levulinic acid up to 40 % for a total conversion was obtained when using S-Mordenite catalyst. This means that sulfonation probably mainly occurred on the external zeolite surface improving the accessibility of the acid centers. The highest selectivity to LA (76 %), achieved by S-βeta (Fig. 4), can be attributed to its higher amount of BrØnsted acid centers, higher external surface area in addition to the higher accessibility of S-βeta, due to the higher flexibility of its structure when compared to S-ZSM-5. This result is comparable to the best catalytic result reported for this reaction using zeolites [28] in which the increase in the mesoporosity of the ZSM-5 zeolite after its treatment with an alkaline solution followed by an acid solution improved the accessibility of the acid sites leading to 76 % of LA yield [28]. In this work, the sulfonic-acid functionalization mainly in the external zeolitic surface increased the amount and improved the accessibility of BrØnsted acid centers.

In addition to levulinic acid, 4-hydroxy-2-cyclopentenone (4-HCP), was detected by gas chromatography for all catalysts with except for H-Mordenite, the less active catalyst. 4-HCP is a by-product caused by the dehydration of the furan ring, which competes with the ring opening for the formation of levulinic acid (Scheme 1), and which is also catalyzed by acid centers. The dehydration reaction was greater for acid-modified ZSM-5 catalysts than for the acid-modified βeta ones, with small differences between protonated and sulfonated forms for each zeolite (Fig. 5). This means that the effect of the acidity strength was not significant for the formation of 4-hydroxy-2-cyclopentenone. However, the higher amount of the acid centers in βeta in addition to their surface and structural properties seems to favor the formation of levulinic acid in front of 4-hydroxy-2-cyclopentenone. The use of H_2 pressure has been previously reported to prevent the formation of furan resins, thus favouring the formation of levulinic acid [27]. In the case of H-Mordenite the entire conversion should be derived from the formation of furan resins, since no ring hydration or other reaction products were detected by GC [21–25].

The stability of the best catalyst, S-βeta, was studied by performing 3 cycles using the reaction conditions of 0.2 g of catalyst at 120 °C, 15 bar H_2 for 1 h (Fig. 6). After each reaction, the catalyst was filtered, washed with the solvent (water/acetone ratio of 1:9) and dried at 80 °C before using for the next run.

Conversion remained complete after 3 cycles. However, a progressive decrease in the selectivity of levulinic acid was observed. To

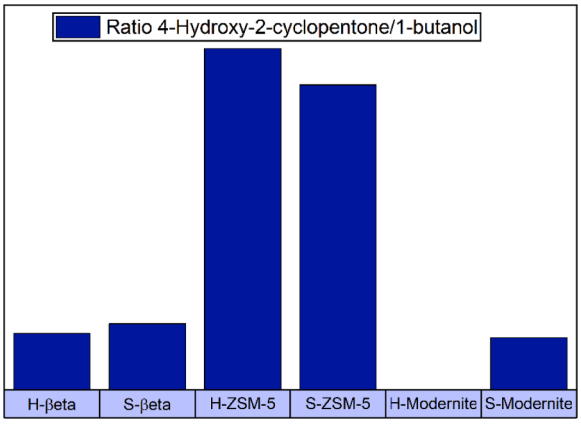

Fig. 5. 4-hydroxy-2-cyclopentenone/internal standard (1-butanol) ratio for all catalysts.

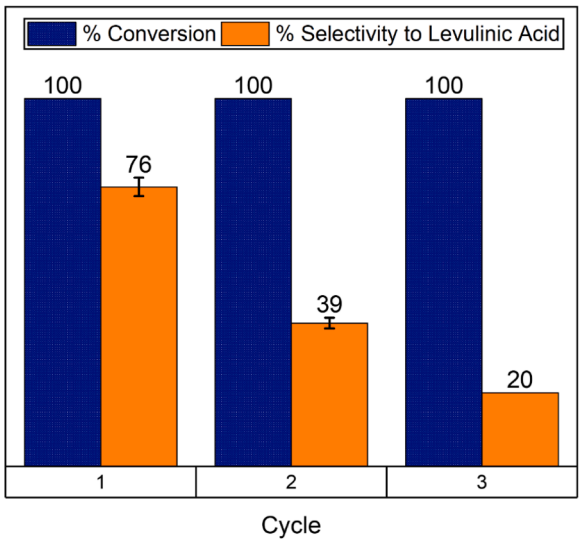

Fig. 6. Reusability of the catalyst S-βeta. Reaction conditions: 0.2 g of catalyst, 120 ºC, 15 bar H_2 for 1 h. Solvent: water/acetone ratio of 1:9. Error bars are indicated for the first and second cycle.

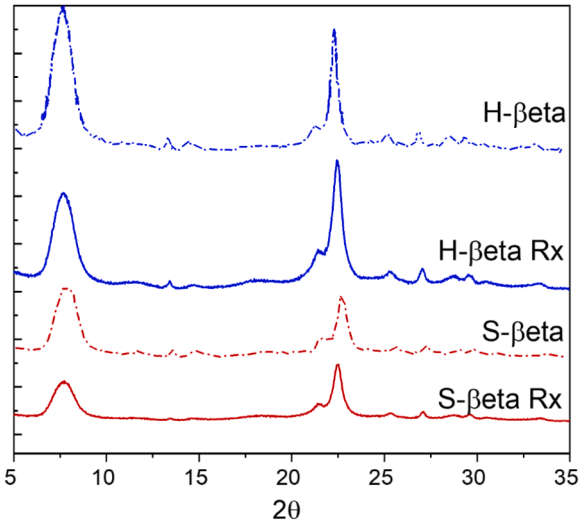

Fig. 7. XRD patterns of the spent (Rx) and fresh catalysts H-βeta and S-βeta.

elucidate what was happening, spent S-βeta catalyst but also H-βeta catalyst were characterized by XRD and TGA techniques to be compared with the corresponding fresh catalysts (Figs. 7 and 8).

XRD patterns did not show practically differences between spent and fresh catalysts (Fig. 7). Therefore, the zeolite structure maintained during the reaction. However, from TGA results a different behavior was observed when comparing the two catalysts. Thus, a significant decrease of weight was detected around 300 ºC for the spent H-βeta catalyst that was not present in the TGA profile of fresh H-βeta (Fig. 8). This should be attributed to the presence of adsorbed reagents or reaction products formed during the reaction, such as humins. Previous studies show that the degradation of biomass-derived humins, characterized by TGA without being supported on any substrate, exhibits mass losses at 210–260 °C. These losses are attributed to the release of low molecular weight compounds present in the polymers, which are formed through condensation or polymerization between fragments—these being the weakest fragments. Another mass loss has been reported between 400–500 °C, which is attributed to the decomposition of the polymer itself [40,41]. Additionally, other authors have reported that poly(furfuryl alcohol) can improve its thermal stability when supported on different materials, such as clays, montmorillonite, or SiO_2, with an increase of 50–100 °C [42,43]. This suggests that the weight loss observed in the catalysts of the current work at 300 °C could be attributed to weak humin fragments, while the loss observed at 550 °C could correspond to the formation of more stable and longer-chain humins. Interestingly, for spent catalyst S-βeta, a lower decrease of weight was observed but at higher temperatures (around 400 ºC) than for the spent H-βeta (Fig. 8). Considering that the loss of sulfonic groups occurred at 360 ºC-660 ºC, as observed in the TGA profile of fresh S-βeta catalyst, sulfonated catalysts, with stronger Brønsted acidity, led to lower amounts of undesired humins. Nevertheless, this complexity hinders the precise attribution of the different signals to specific types of humins or sulfur-containing groups. However, the shift of sulfonic groups to lower temperatures, along with the absence of a peak at 300 °C, suggests a significant presence of low molecular weight compounds attached to the active centers of the catalyst. Furthermore, a slight weight loss observed at 700 °C may be associated with the presence of longer-chain humins. These TGA results could explain the decrease in the selectivity to LA observed during reuse of S-βeta (Fig. 6), as the humins formed exhibit increased thermal stability due to their strong interaction with active sites, limiting their degradation and potential removal. The sulfur content was similar for the fresh and used catalyst, as determined by SEM-EDX, confirming that the presence of humins should be the responsible for catalyst deactivation. Therefore, washing of the spent catalyst with the solvent was not enough to remove these adsorbed compounds.

In order to improve the reuse, and eliminate the adsorbed organic compounds, the spent catalyst H-βeta was calcined at 400 ºC during 3 h before its reuse. The catalytic result (Fig. 9a) showed a slight decrease of

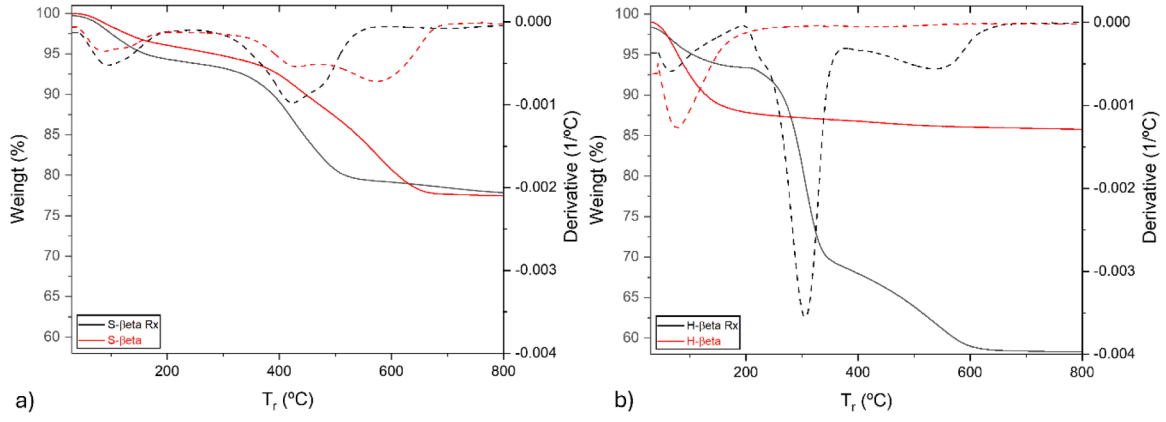

Fig. 8. TGA profiles of the spent (Rx) and fresh catalysts a) S-βeta and b) H-βeta. Dashed lines are the corresponding derivatives.

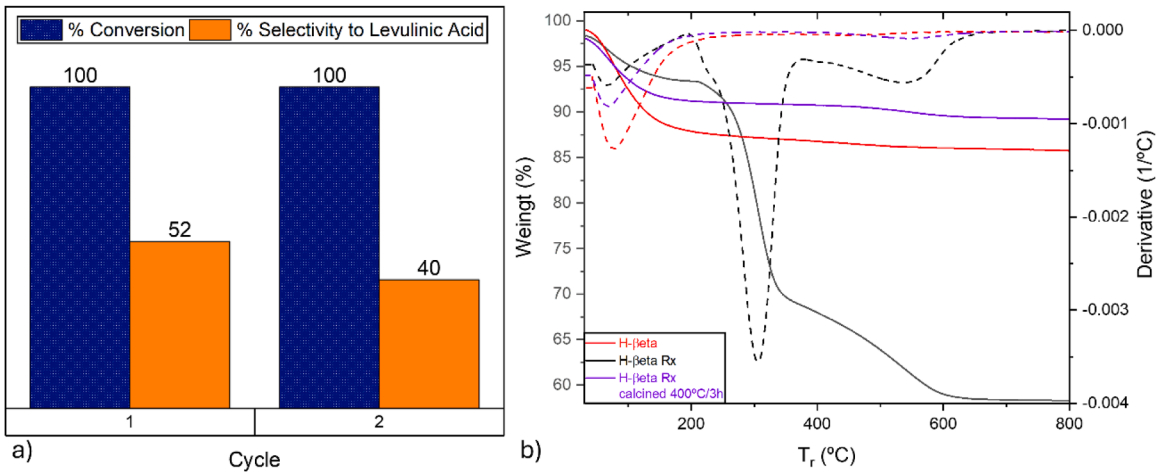

Fig. 9. a) Catalytic activity result of spent catalyst H-βeta. Reaction conditions: 0.2 g of catalyst, 120 °C, 15 bar H_2 for 1 h. Solvent: water/acetone ratio of 1:9.; b) TGA profile of the spent catalyst H-βeta after calcination at 400 °C for 3 h, compared to the fresh one. Dashed lines are the corresponding derivatives.

the selectivity to LA in the second cycle according to the TGA profile of the spent H-βeta after calcination at 400 °C during 3 h (Fig. 9b), in which no weight loss at 300 °C was observed.

Therefore, calcination at moderate temperatures can eliminate the products retained during reaction increasing the catalytic life of the zeolite catalyst. This methodology for reactivating the catalyst could not be applied for S-βeta since the calcination process would eliminate partially the sulfonic groups, responsible for the catalytic activity. The adsorption of the organic compounds was not irreversible, so other catalyst cleaning methodologies or reactivation methods should be developed for sulfonated catalysts to increase their recyclability.

4. Conclusions

Protonated and sulfonic-acid functionalized βeta, ZSM-5 and Mordenite zeolites were active for the selective obtention of levulinic acid from furfuryl alcohol with the exception of H-Mordenite. A mixture of acetone/water was used during reaction as greener solvent. Sulfonated zeolites led to higher selectivity to levulinic acid than H-zeolites due to the higher amount, strength and accessibility of their BrØnsted acid sites. Sulfonated zeolites maintained the zeolitic structure although some loss of crystallinity and partial dealumination was observed, especially for S-βeta and S-Mordenite. The null selectivity to levulinic acid obtained for H-Mordenite increased up to 40 % for S-Mordenite due to the higher amounts and especially accessibility of the BrØnsted acid sites generated after sulfonic-acid treatment, which probably was mainly produced on the external surface. The highest selectivity to LA (76 %) was achieved by S-βeta for a total conversion. This can be attributed to its higher amount of BrØnsted acid centers, higher external surface area and higher accessibility of βeta zeolite, which has a more flexible structure. Additionally, ZSM-5catalysts led to higher amounts of 4-hydroxy-2-cyclopentenone, an undesirable by-product, than βeta and Mordenite catalysts. H-βeta showed higher stability in the reuse than S-βeta because the deactivating products adsorbed during reaction can be eliminated by calcination.

CRediT authorship contribution statement

CESTEROS YOLANDA: Writing – review & editing, Writing – original draft, Validation, Supervision, Resources, Funding acquisition, Conceptualization. **Le Corre Adrien:** Methodology, Investigation, Conceptualization. **Fuentes-Rodríguez Laura:** Writing – original draft, Visualization, Validation, Methodology, Investigation, Data curation.

Declaration of Competing Interest

The authors declare that they have no known competing financial interests or personal relationships that could have appeared to influence the work reported in this paper.

Acknowledgments

This work was supported by the project TED2021–129487B-C31 funded by MICIU/AEI/10.13039/501100011033, European Union NextGenerationEU/PRTR and NextGenerationEU/Catalunya 2023 INV-2 00033-ID11.

Data availability

The data that has been used is confidential.

References

[1] S.K. Sansaniwal, K. Pal, M.A. Rosen, S.K. Tyagi, Renew. Sustain. Energy Rev. 72 (2017) 363–384, https://doi.org/10.1016/j.rser.2017.01.038.
[2] H. Li, A. Riisager, S. Saravanamurugan, A. Pandey, R.S. Sangwan, S. Yang, R. Luque, ACS Catal. 8 (2018) 148–187, https://doi.org/10.1021/ACSCATAL.7B02577.
[3] C. Xu, E. Paone, D. Rodríguez-Padrón, R. Luque, F. Mauriello, Renew. Sustain. Energy Rev. 127 (2020) 109852, https://doi.org/10.1016/j.rser.2020.109852.
[4] T. Werpy, J. Holladay, J. White, 2004, Top value added chemicals from biomass: I. Results of screening for potential candidates from sugars and synthesis gas, 2004. https://doi.org/10.2172/15008859..
[5] K. Yan, C. Jarvis, J. Gu, Y. Yan, Renew. Sustain. Energy Rev. 51 (2015) 986–997, https://doi.org/10.1016/j.rser.2015.07.021.
[6] W. Ouyang, D. Zhao, Y. Wang, A.M. Balu, C. Len, R. Luque, ACS Sustain. Chem. Eng. 6 (2018) 6746–6752, https://doi.org/10.1021/ACSSUSCHEMENG.8B00549.
[7] Y. Lu, Y. Wang, Q. Tang, Q. Cao, W. Fang, Appl. Catal. B Environ. 300 (2022) 120746, https://doi.org/10.1016/j.apcatb.2021.120746.
[8] D.R. Chaffey, T. Bere, T.E. Davies, D.C. Apperley, S.H. Taylor, A.E. Graham, Appl. Catal. B Environ. 293 (2021) 120219, https://doi.org/10.1016/j.apcatb.2021.120219.
[9] D. Unlu, N. Boz, O. Ilgen, N. Hilmioglu, Open Chem. 16 (2018) 647–652, https://doi.org/10.1515/CHEM-2018-0070.
[10] A. Khoshsima, D. Brock, D. Touraud, W. Kunz, Fuel 191 (2017) 212–220, https://doi.org/10.1016/j.fuel.2016.11.075.
[11] J. Wang, J. Zhang, J. Li, M.M. Dawuda, B. Ali, Y. Wu, J. Yu, Z. Tang, J. Lyu, X. Xiao, L. Hu, J. Xie, Front. Plant Sci. 12 (2021) 683868, https://doi.org/10.3389/FPLS.2021.683868.
[12] Y. Wu, N. Liu, L. Hu, W. Liao, Z. Tang, X. Xiao, J. Lyu, J. Xie, A. Calderón-Urrea, J. Yu, Front. Plant Sci. 12 (2021) 636121, https://doi.org/10.3389/FPLS.2021.636121.
[13] Z. Min Zhan, H. Qiang Yan, P. Yin, J. Cheng, Z. Ping Fang, Polym. Int. 69 (2020) 355–362, https://doi.org/10.1002/PI.5957.
[14] L.G. Covinich, N.M. Clauser, F.E. Felissia, M.E. Vallejos, M.C. Area, Biofuels, Bioprod. Bioref. 14 (2020) 417–445, https://doi.org/10.1002/BBB.2062.

[15] A. Morone, M. Apte, R.A. Pandey, Renew. Sustain. Energy Rev. 51 (2015) 548–565, https://doi.org/10.1016/j.rser.2015.06.032.
[16] B.C. RedmonProcess for the production of levulinic acid, US patent 2738367, 1956..
[17] K. Tsukuru, H. Yoshio, M. Takesi, O. MasatomiManufacture of levulinic acid, US patent 3752849, 1973..
[18] W. Van De Graaf, J.P. LangeProcess for the conversion of furfuryl alcohol into levulinic acid or alkyl levulinate, US Patent 20070049771, 2007..
[19] B. Capai, G. Artigau, Prep. levulinic Acid. (1992). US patent 5175358,.
[20] J. Bozell, L. Moens, D. Elliott, Y. Wang, Resour., Conserv. Recycl 28 (2000) 227–239, https://doi.org/10.1016/S0921-3449(99)00047-6.
[21] T. Kim, R. Assary, H. Kim, C. Marshall, D.J. Gosztola, L.A. Curtiss, P.C. Stair, Catal. Today 205 (2013) 60–66, https://doi.org/10.1016/j.cattod.2012.09.033.
[22] T. Kim, R. Assary, R.E. Pauls, C.L. Marshall, L.A. Curtiss, P.C. Stair, Catal. Commun. 46 (2014) 66–70, https://doi.org/10.1016/j.catcom.2013.11.030.
[23] M.G. Alimukhamedov, F.A. Magrupov, Polym. Sci. - Ser. B 49 (2007) 167–171, https://doi.org/10.1134/S1560090407070019.
[24] I. Chuang, G. Maciel, G.E. Myers, Macromol 17 (1984) 1087–1090, https://doi.org/10.1021/ma00135a019.
[25] T. Krishnan, M. Chanda, D*ie*, Angew. Makromol. Chem. Appl. Macromol. 43 (1975) 145–146, https://doi.org/10.1002/apmc.1975.050430110.
[26] M.A. Mellmer, J.M.R. Gallo, D. Martin Alonso, J.A. Dumesic, ACS Catal. 5 (2015) 3354–3359, https://doi.org/10.1021/acscatal.5b00274.
[27] I. Guzmán, A. Heras, M.B. Güemez, A. Iriondo, J.F. Cambra, J. Requies, Ind. Eng. Chem. Res. 55 (2016) 5139–5144, https://doi.org/10.1021/acs.iecr.5b04190.
[28] P. Yan, H. Wang, Y. Liao, P. Sun, C. Wang, Fuel 329 (2022) 125213, https://doi.org/10.1016/j.fuel.2022.125213.
[29] R. Wang, F. Shen, Y. Tang, H. Guo, R. Lee Smith, X. Qi, Renew. Energy 171 (2021) 124–132, https://doi.org/10.1016/j.renene.2021.02.064.
[30] C. Breen, Clay Min. 26 (1991) 487–496, https://doi.org/10.1180/CLAYMIN.1991.026.4.04.
[31] R. Mokaya, W. Jones, S. Moreno, G. Poncelet, Catal. Lett. 49 (1997) 87–94, https://doi.org/10.1023/A:1019084617120.
[32] J.A. Ballantine, J.H. Purnell, J.M. Thomas, Clay Min. 18 (1983) 347–356, https://doi.org/10.1180/CLAYMIN.1983.018.4.02.
[33] J.H. De Boer, The Structure and Properties of Porous Materials, Butterworth, London, 1958.
[34] W. Zhang, X. Wang, Z. Wu, Z. Li, X. Yong, Y. Gu, J. Wang, Catal. Sci. Technol. 14 (2024) 1760–1774, https://doi.org/10.1039/d3cy01558k.
[35] P.A. Jacobs, H.K. Beyer, J. Valyon, Zeolites 1 (1981) 161–168, https://doi.org/10.1016/S0144-2449(81)80006-1.
[36] J.M. Newsam, M.M. Treacy, W.T. Koetsier, C.B. de Gruyter, Proc. R. Soc. Lond. A. Math. Phys. Sci. 420 (1988) 375–405, https://doi.org/10.1098/rspa.1988.0131.
[37] M. Müller, G. Harvey, R. Prins, Microporous Mesoporous Mater. 34 (2000) 135–147, https://doi.org/10.1016/S1387-1811(99)00167-5.
[38] M.D. González, Y. Cesteros, P. Salagre, Microporous Mesoporous Mater. 144 (2011) 162–170, https://doi.org/10.1016/J.MICROMESO.2011.04.009.
[39] S. Moreno, G. Poncelet, Microporous Mater. 12 (1997) 197–222, https://doi.org/10.1016/S0927-6513(97)00067-9.
[40] S.J.C. Gariboti, M. Gontijo, E.L. Gomes, Y.J. Rueda-Ordóñez, R. Fernandez, L. Plazas, JAAP 166 (2022) 105605, https://doi.org/10.1016/j.jaap.2022.105605.
[41] P. Tosi, G. vanKlink, A. Celzard, L. Fierro, E. Vincent, A. deJong, Mija, ChemSusChem 11 (2018) 2797–2809, https://doi.org/10.1002/cssc.201800778.
[42] S.D.E. Kherroub, M. Belbachir, S. Lamouri, Bull. Mater. Sci. 38 (2015) 57–63, https://doi.org/10.1007/s12034-014-0818-3.
[43] N. Guigo, A. Mija, R. Zavaglia, L. Vincent, N. Sbirrazzuoli, Polym. Degrad. Stabil. 94 (2009) 908–913, https://doi.org/10.1016/j.polymdegradstab.2009.03. . 008.